ACS APPLIED MATERIALS & INTERFACES

Research Article

www.acsami.org

# Study of Hole-Injecting Properties in Efficient, Stable, and Simplified Phosphorescent Organic Light-Emitting Diodes by Impedance Spectroscopy

S. D. Cai, C. H. Gao, D. Y. Zhou, W. Gu, and L. S. Liao*

Jiangsu Key Laboratory for Carbon-Based Functional Materials & Devices, Institute of Functional Nano & Soft Materials (FUNSOM), Soochow University, Suzhou, Jiangsu 215123, China

Supporting Information

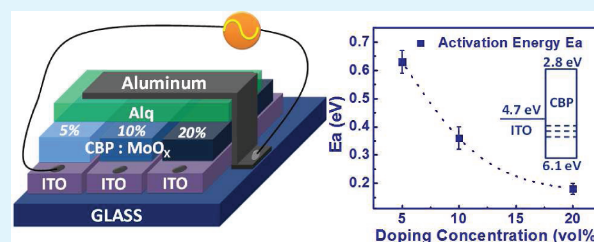


**ABSTRACT:** Simplified phosphorescent organic light-emitting diodes (OLEDs) using only two kinds of hosts and comprising either a neat $MoO_x$ hole-injecting layer (HIL) or a $MoO_x$-doped 4,4′-bis(carbazol-9-yl)biphenyl (CBP) HIL were studied. The devices having the $MoO_x$-doped CBP HIL are superior to the device having the neat $MoO_x$ HIL in terms of power efficiency and operational lifetime. Impedance spectroscopy studies revealed that both the reduced hole-injecting barrier height at the anode/doped HIL interface and the reduced bulk resistivity in the doped CBP HIL contribute to the improvement in electroluminescence characteristics. When increasing the $MoO_x$ volume percentage from 5 to 10% and then to 20%, the hole-injecting barrier height is decreased from 0.63 eV to 0.36 eV and then to 0.18 eV. The power efficiency of the device with a 20 vol % of $MoO_x$-doped CBP HIL is more than two times that of the device with a neat $MoO_x$ HIL measured at a driven current of 5 mA/cm$^2$. Moreover, the lifetime of the device with a 20 vol % of $MoO_x$-doped CBP HIL is more than three times that of the device with a neat $MoO_x$ HIL estimated at an initial luminance of 1000 cd/m$^2$. The $MoO_x$-doped HIL further ensures the feasibility of the simplified phosphorescent OLEDs for potential applications.

**KEYWORDS:** *phosphorescent OLEDs, doped hole-injecting layer, hole injection properties, impedance spectroscopy, $MoO_x$, electroluminescence characteristics*

## 1. INTRODUCTION

To achieve high efficiency in organic light-emitting diodes (OLEDs), phosphorescent OLEDs (PHOLEDs) with a theoretical value of 100% internal quantum efficiency are attracting intensive attention.[1−7] A high-efficiency PHOLED generally has many functional layers including hole-injecting layer (HIL), hole-transporting layer (HTL), exciton-blocking layer, light-emitting layer (LEL), hole-blocking layer, electron-transporting layer, and electron-injecting layer. Recently, Meyer et al. and Wang et al., reported high efficiency PHOLEDs with highly simplified layer structures containing only two host materials,[5−7] TCTA with TPBI, or CBP with TPBI, where TCTA is 4,4′,4″-tris(N-carbazolyl)-triphenyl amine, CBP is 4,4′-bis(carbazol-9-yl)biphenyl, and TPBI is 2,2′,2″-(1,3,5-benzine-triyl)-tris(1-phenyl-1-H-benzimidazole). The TCTA and CBP are the hole-transporting materials, and the TPBI is the electron-transporting material. Light emission comes either from doped electron-transporting material (in the device of TCTA | TPBI) or doped hole-transporting material (in the devices of CBP | TPBI). These simplified PHOLED structures can obviously save fabrication cost and will be potentially useful to real applications. However, due to the lower HOMO level of TCTA layer or CBP layer, which is more than 6.0 eV below the vacuum energy level,[5−8] it is a challenge to form a low or no hole-injection barrier at the interface between the anode and the HTL in the simplified PHOLEDs. Fortunately, a thin layer of metal oxide, such as $WO_3$ and $MoO_3$, as the HIL or a chlorinated indium tin oxide (ITO) as the anode have been reported useful in the simplified PHOLEDs.[5−7] However, it has not yet been reported that whether or not a neat $MoO_x$ ($2 \leq x \leq 3$) HIL is superior to other HIL, such as to a doped HIL, in terms of efficiency and lifetime in the simplified PHOLEDs. In our work we found that, if we form a $MoO_x$-doped CBP HIL instead of forming a neat $MoO_x$ HIL in the simplified PHOLEDs, the electroluminescence (EL) performance of the devices containing the doped HIL can be substantially improved. Therefore, here in this paper, we show the difference of the simplified PHOLEDs containing either a neat $MoO_x$ HIL or a $MoO_x$-doped CBP HIL, and then study their hole-injection properties in the simplified devices by impedance spectroscopy (IS).

## 2. EXPERIMENTAL SECTION

In our experiments, five phosphorescent green-emitting diodes were fabricated for EL comparison. The device structures are "ITO | HIL | HTL | CBP:$Ir(ppy)_2(acac)$ (8 vol %) (15 nm) | TPBI (65 nm) | LiF (0.5 nm) | Al (100 nm)", where the HIL | HTL are "CBP: $MoO_x$ (0, 5,

Received: October 3, 2011
Accepted: November 28, 2011
Published: November 28, 2011

 © 2011 American Chemical Society 

10, 20 vol %) (25 nm) | CBP (10 nm)" which are denoted as devices A(0), A(5), A(10), and A(20), and "$MoO_x$ (1 nm) | CBP (35 nm)" as device A(Neat), respectively. The organic material $Ir(ppy)_2(acac)$ is bis(2-phenylpyridine)(acetylacetonate)iridium(III). For temperature-dependent IS measurement, three hole-only transport devices, B(5), B(10), and B(20), were fabricated as "ITO | CBP: $MoO_x$ (5, 10, 20 vol %) (60 nm) | tris(8-hydroxyquinoline) aluminum(III) (Alq) (60 nm) | Al (100 nm)", respectively. In addition, five double-layer devices, C(0), C(5), C(10), C(20), and C(Neat) were made with the structures of "ITO | CBP: $MoO_x$ (0, 5, 10, 20 vol %) (50 nm) | CBP (50 nm) | Al (100 nm)" and "ITO | $MoO_x$ (1 nm) | CBP (100 nm) | Al (100 nm)", respectively. Moreover, two single-layer devices, D(10), and D(Neat) were formed with the structures of "ITO | CBP: $MoO_x$ 10 vol % (150 nm) | Al (100 nm)" and "ITO | $MoO_x$ (1 nm) | CBP (150 nm) | Al (100 nm)", respectively. Both the double-layer devices and the single-layer devices were used for current−voltage ($I-V$) measurements, IS measurement, equivalent circuit simulation, as well as for diffusion length test. All the materials used in this work are as-received with the purity higher than 99%, among which $MoO_x$ powder was purchased from Aldrich with a nominal "$x$" value equal to 3 but a tested "$x$" value of an evaporated film equal to about 2.8 according to our X-ray photoelectron spectroscopy studies. The samples were fabricated on glass substrates with an ITO thickness of ∼100 nm and a sheet resistance of ∼30 Ω per square. The active area of each device is 0.1 $cm^2$ (0.33 mm × 0.3 mm). The deposition rates and doping concentrations of materials were controlled and measured in situ using calibrated thickness monitors. The deposition rate of the organic host materials was 0.4 nm/s, and the deposition rates of the dopant materials were adjusted according to the volume ratio in the host materials. The Al cathode formed on top of the organic layers has a thickness of about 100 nm. After the deposition, the devices were transferred from the vacuum chamber into a nitrogen-filled glovebox for encapsulation before testing. The $I-V$ and luminance characteristics were measured using Keithley 2400s source meter and Photo Research PR655 spectrophotometer. The IS measurements were performed using Wayne Kerr 6550B precision impedance analyzer with 30 mV perturbation oscillation signal in a frequency range from 50 Hz to 20 MHz. The samples for IS measurements were amounted in a LakeShore probe station and tested in a temperature range of from 80 to 340 K. The diffusion lengths of $MoO_x$ in CBP layer were estimated according to the parallel capacitances measured by an Aglient 4096A digital oscilloscope and a Tabor 8551 functional signal generator.

## 3. RESULTS AND DISCUSSION

**Electroluminescence and Lifetime.** Shown in Figure 1 are the EL characteristics of devices A(0), A(5), A(10), A(20), and A(Neat). Figure 1a shows the $I-V$ characteristics of the devices. With the increase of $MoO_x$ doping concentration from 0 to 20 vol %, the current density is substantially increased at each specific voltage. For example, at a bias of +6 V, the current density passing through devices A(0), A(5), A(10), and A(20) is rapidly increased and results in at least 1 order of magnitude in difference between device A(0) and device A(20). Although it has better I−V characteristics than device A(0), device A(Neat) is inferior to the other $MoO_x$-doped devices according to the I−V performance in our experiments. The inset of Figure 1a shows the normalized EL spectra of device A(20) operated at the current density of 0.1, 1, 10, and 40 mA/$cm^2$, respectively. No peak shift is observed from the spectra, which indicates that the radiation recombination in the LEL is well confined at the HTL/LEL interface. Figure 1b shows the power efficiency vs current density of the devices. Similar to Figure 1a, with the increase of the $MoO_x$ doping concentration from 0 to 20 vol %, the power efficiency is substantially increased as well. At 5 mA/$cm^2$, the power efficiencies are 18, 34, 54, and 63 lm/W for devices A(0), A(5), A(10), and A(20),

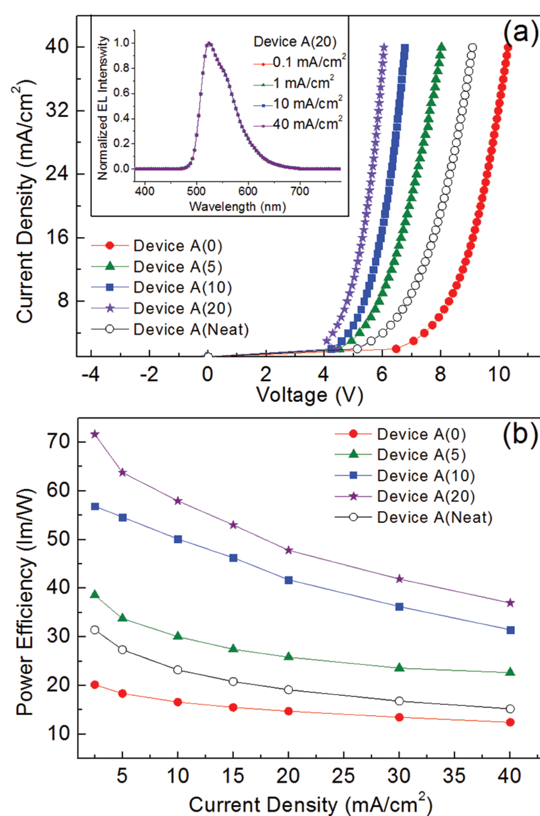


**Figure 1.** EL characteristics of devices A(0), A(5), A(10), A(20), and A(Neat). (a) $I-V$ characteristics of the devices. The inset shows the normalized EL spectra of device A(20) operated at the current density of 0.1, 1, 10, and 40 mA/$cm^2$, respectively. (b) Power efficiency vs current density of the devices. Devices A(0), A(5), A(10), and A(20) have a $MoO_x$-doped CBP HIL with the doping concentration of 0, 5, 10, and 20 vol %, respectively, and A(Neat) has a neat $MoO_x$ HIL with 1 nm in thickness.

respectively (The power efficiency vs $MoO_x$ doping concentration in the CBP layer is shown in Figure S1 in the Supporting Information and the current efficiency vs current density of the devices can be seen in Figure S2 in the Supporting Information). Although it has a better power efficiency than device A(0), device A(Neat) is also inferior to the other $MoO_x$-doped devices in terms of the efficiency in our experiments. For example, the power efficiency of device A(20), 63 lm/W, is more than two times that of device A(Neat), 28 lm/W, measured at a driven current of 5 mA/$cm^2$.

As for devices A(0) and A(Neat), the layer structures of the two devices are the same except that A(Neat) has a 1-nm-thick $MoO_x$ layer. This 1-nm-thick $MoO_x$ layer was added to modify the ITO surface for reducing hole-injecting barrier height. To understand the effect of the thin $MoO_x$ layer on the hole-injecting barrier, we made two devices, device E(Neat) with the layer structure of ITO | $MoO_x$ | CBP | Al and device E(0) with the layer structure of ITO | CBP |Al, for built-in potential comparison. Photovoltaic measurements of the two devices indicated that the built-in potential of the device with $MoO_x$ layer is about 0.4 V higher than that of the device without $MoO_x$ layer (shown in Figure S3 in the Supporting Information). The difference of built-in potential between A(Neat) and A(0) should be the same as that between E(Neat) and E(0). The built-in potential is considered to result from the difference between the work functions of the anode and the

cathode.[9] Therefore, the difference of built-in potential in A(Neat) and A(0) indicates that the hole injection barrier of A(Neat) at the anode interface is indeed about 0.4 eV lower than that of device A(0). As a result, the EL characteristics of A(Neat) are better than that of A(0).

The lifetime data shown in Figure 2 indicate that device A(Neat) has a shorter lifetime than A(20) in our experiments

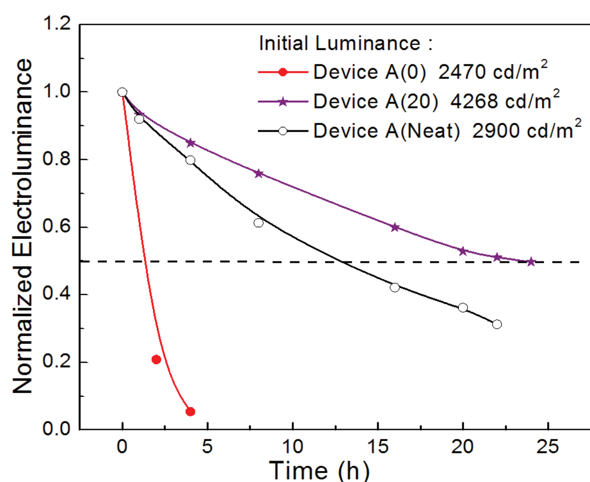


**Figure 2.** Normalized EL vs operational time of devices A(0), A(20), and A(Neat), tested at room temperature and at 5 mA/cm$^2$.

measured at 5 mA/cm$^2$. For easy comparison, the measured lifetime at different initial luminance can be converted into the same luminance by an empirical equation[10]

$$T_{50}(L) = T_{50}(L_0)\left(\frac{L_0}{L}\right)^{1.5} \tag{1}$$

where $T_{50}(L)$ is the lifetime being converted at an initial luminance of $L$ cd/m$^2$, $T_{50}$ ($L_0$) is the real lifetime at the initial luminance of $L_0$. According to the empirical equation, the comparable lifetime at the initial luminance of 1000 cd/m$^2$ is about 8, 64, and 212 h for devices A(0), A(Neat), and A(20), respectively. Therefore, the $MoO_x$-doped HIL exhibits substantial improvement on lifetime over the neat $MoO_x$ HIL in the simplified PHOLEDs.

There are many factors to affect the lifetime of OLEDs, especially PHOLEDs. Using the $MoO_x$-doped CBP layer is one of many ways to improve the anode interface and to enhance the device lifetime.[11] If the other interfaces could also be carefully designed with suitable materials and layer structures, the lifetime of the devices would be further increased.

As is known, devices A(0), A(5), A(10), A(20), and A(Neat) are structurally identical except the difference in the HIL. Thus, the difference in EL performance should be related to both the hole-injection barrier at the anode/HIL interface and the property of the bulk HIL.

**Impedance Spectroscopy Investigation.** To investigate the hole-injection barrier at the anode/HIL interface of the studied devices, we made devices B(5), B(10), and B(20) for IS measurement. Actually, IS measurement is a very useful method to study electrical properties of electronic devices.[12−18] The details of the IS measurement for the study of hole-injection barrier have been reported by Hsieh et al.[13,14] Considering the energy barrier between the Alq layer and the aluminum cathode, as well as the very low oscillation level, these devices can be treated as hole-only devices.[15,17] Moreover, each layer in the devices can be treated as an RC element according to the IS theory.[18] However, because the parallel resistance of 60 nm Alq layer is much larger than that of the doped CBP layer in the devices, the RC element of the CBP layer can be treated as only a capacitor. Thus the inflection frequency related to the CBP layer can be described as

$$\omega = \tau^{-1} = R_{CBP}(C_{CBP} + C_{Alq}) \tag{2}$$

Shown in Figure 3 are the temperature-dependent dC/dF-F spectra of the devices, measured at zero bias. In Figure 3a−c,

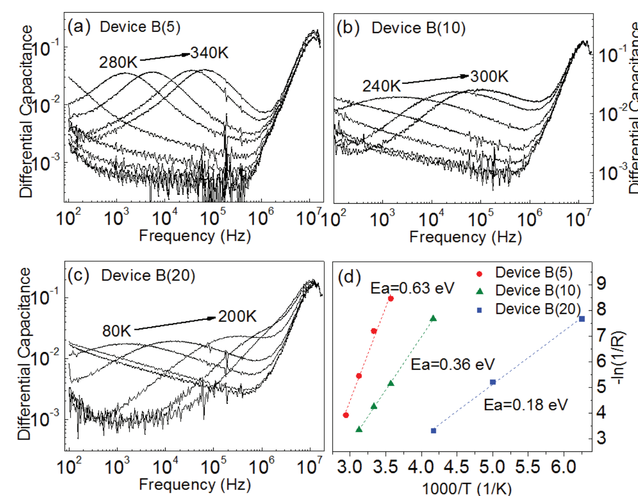


**Figure 3.** Temperature-dependent dC/dF-F spectra at zero bias for devices (a) B(5), (b) B(10), and (c) B(20), and the derived data: (d) plots of $-\ln(1/R)$ vs $1000/T$.

there are two distinct peaks corresponding to two inflection frequencies in the spectra, one is related to the resistance of the CBP layer as the low-frequency peak and the other is mainly related to the lead resistance or electrical contact resistance as the high-frequency peak. Based on the data shown in Figure 3a−c, the hole-injection barrier height or the activation energy $E_a$ (= $E_F - E_{HOMO}$) of each device can be derived from the curve of $-\ln(1/R_{CBP})$ vs $1000/T$ as shown in Figure 3d. When increasing the $MoO_x$ volume percentage from 5 to 10% and then to 20%, the activation energy is decreased from 0.63 eV to 0.36 eV and then to 0.18 eV. Therefore, if we relate the activation energy to the EL performance of the $MoO_x$-doped devices, we could clearly see that the decrease in activation energy does increase the power efficiency accordingly. As for device A(Neat), although the LUMO level (empty states) of $MoO_3$ is reported in the range of from 5.7 to 6.7 eV, there still exists a hole-injection barrier between a neat $MoO_3$ layer and the adjacent HTL due to Fermi level pinning that is originated from electron transfer between the HOMO of the HTL and the low-lying unoccupied states of $MoO_3$.[19−21] The EL performance of A(Neat) confirms that an hole-injection barrier does existed, which should be higher than that of device A(5) (At least 0.3 eV higher).

Therefore, our experimental data show that the hole-injection barrier height of both the $MoO_x$-doped HIL and the neat $MoO_x$ HIL controls the EL performance in the simplified PHOLEDs. The lower the hole-injection barrier, the higher the luminous efficiency of the devices.


dx.doi.org/10.1021/am2013568 | ACS Appl. Mater. Interfaces 2012, 4, 312−316

**Diffusion Length.** In addition to the injection barrier, the bulk resistance in the $MoO_x$-doped HIL should also affect the EL performance of the devices. Shown in Figure 4 are the capacitances of devices C(0), C(5), C(10), C(20), and C(Neat) measured at 10 kHz with both a 4 V triangle waveform and a 50 ohm inner resistor load. When the amplitude of the triangle voltage is lower than 2 V, the capacitances of C(0), C(5), C(10), C(20), and C(Neat) are 2.5, ~5.0, 5.3, 5.7, and 2.7 nF, respectively. (Because of the low doping concentration in device C(5), the doped CBP layer may not be completely short circuited under a low bias voltage of less than 2 V, which results in a gradual increase in capacitance.) The geometrical capacitances can be used to estimate the thickness of the dielectric layer (i.e., the neat CBP layer here) according to a commonly known equation of the geometrical capacitance.[16] In the deposition process, the thicknesses of the deposited layers are precisely controlled by a thickness monitor. C(0) has the capacitance of 2.5 nF, which corresponds to 100 nm thick CBP layer. Thus, 5.0, 5.3, 5.7, and 2.7 nF correspond to 50, 47, 44, and 93 nm of CBP thickness in devices C(5), C(10), C(20), and C(Neat), respectively. From electrical conduction point of view, the $MoO_x$-doped CBP layers in the parallel capacitors are electrically shorted with high conductivity. Therefore, device C(20) has 44 nm undoped CBP layer with 56 nm $MoO_x$-doped CBP layer, indicating that the original thickness of the doped layer has been broadened from 50 to 56 nm resulting from $MoO_x$ diffusion. Thus the diffusion length was estimated as 6 nm in device C(20). Similarly, the diffusion lengths were estimated as 0, 3, and 7 nm, respectively, in devices C(5), C(10), and C(Neat). It is a great advantage that the $MoO_x$-doped HIL is electrically conductive to reduce drive voltage and improve hole transport in the devices. The conductive characteristics of the $MoO_x$-doped HIL certainly enhance the EL performance of the simplified PHOLEDs.

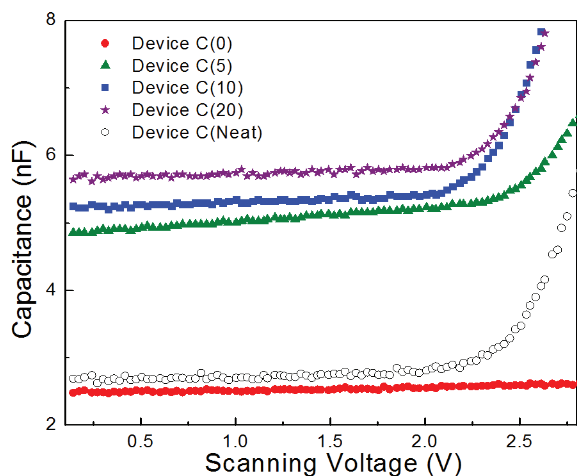


**Figure 4.** Capacitance vs forward-scanning voltage with a triangle waveform and a frequency of 10 kHz on device C(0), C(5), C(10), C(20), and C(Neat), respectively.

**Cole−Cole Plot and Simulation.** To quantitatively compare the enormous difference in resistivity between the neat CBP layer and the doped-CBP layer, we measured the impedance of devices D(Neat), D(5), D(10), and D(20), respectively. Because the "cole−cole" plot shapes of devices D(5), D(10), and D(20) are the same (but with different resistance values under a certain bias), we just selected those of device D(10) to represent the doped CBP layer. Shown in Figure 5 are the cole−cole plots of both the measured and the simulated results of devices D(Neat) and D(10). Precise simulation can be achieved using a $R_s(R_pC_p)$ model and a $R_s(R_{p1}CPE_1)$ $(R_{p2}CPE_2)$ model[17,22] (CPE is an abbreviation of constant phase element) to respectively fit the measured curves of devices D(Neat) and D(10). The impedance of a CPE can be described by $Z(\omega) = Q(j\omega)^{-\alpha}$, where $Q$ is a constant parameter and the value of $\alpha$ changes between 0 to 1. When $\alpha$ = 1, the CPE is like a regular capacitor. The accurate electrical element parameters can also be obtained over a wide bias and frequency range. The detail simulated values are shown in Table 1. The capacitance value almost does not change in a bias range from 0 to 6 V in device D(Neat). Under the bias of 0.5 V, the bulk resistance $R_p$ in the device is about $2 \times 10^7$ ohm. The cole−cole plots shown in Figure 5b are different from those in Figure 5(a). Two semicircles are discernible in each plot. According to the $R_s(R_{p1}CPE_1)$ $(R_{p2}CPE_2)$ model, the two semicircles represent two regions. One is an organic conductive region near the ITO side, and the other is a depletion region near the cathode.[23] The existence of a depletion region at the metal interface implies that the $MoO_x$-doped CBP layer does contain free carriers. Because there are free carriers in the doped layer, the total bulk resistance ($R_{p1}$ and $R_{p2}$) of device D(10) is dramatically reduced to ~500 ohm under the bias of 0.5 V, which is 4 orders of magnitude lower than that of device D(Neat). Therefore, the results further confirm that the improved EL performance of the devices containing $MoO_x$-doped CBP layer indeed relates to the improvement of the bulk conductivity of the HIL layer in the simplified PHOLEDs.

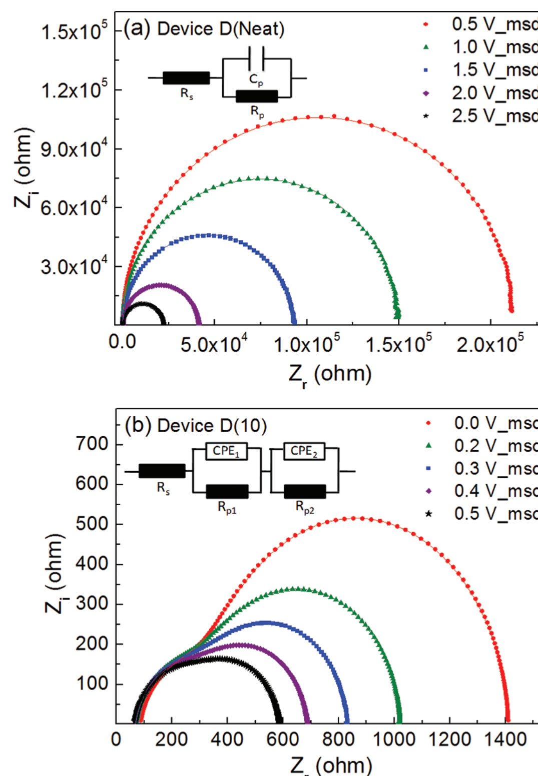


**Figure 5.** Cole−Cole plots of (a) device D(Neat) tested at the bias of 0.5, 1.0, 1.5, 2.0, and 2.5 V, respectively, and (b) device D(10) tested at 0.0, 0.2, 0.3, 0.4, 0.5 V, respectively.

**Table 1. Device Parameters of $R_s(R_pC_p)$ Model and $R_s(R_{p1}CPE_1)$ $(R_{p2}CPE_2)$ Model Used to Simulate the Measured Cole−Cole Plots of Device D(Neat) and D(10) in Figure 5, Respectively**

| | *D*(Neat) | | | | |
|---|---|---|---|---|---|
| | 0.5 V | 1 V | 1.5 V | 2 V | 2.5 V |
| $R_s$ (Ω) | 63.01 | 57.19 | 59.66 | 58.06 | 60.3 |
| *C* (F) | $4.93 \times 10^{-10}$ | $4.92 \times 10^{-10}$ | $4.89 \times 10^{-10}$ | $4.88 \times 10^{-10}$ | $4.86 \times 10^{-10}$ |
| *R* (Ω) | 2.12E7 | 1.492E7 | 9.251E4 | 4.12E4 | 2.22E4 |
| | D(10) | | | | |
| | 0.0 V | 0.2 V | 0.3 V | 0.4 V | 0.5 V |
| $R_s$(Ω) | 85.21 | 69.51 | 68.21 | 66.95 | 65.71 |
| $CPE_1$:$Q_1/\alpha_1$ | $3.34 \times 10^{-8}$/0.963 | $4.22 \times 10^{-8}$/0.948 | $4.98 \times 10^{-8}$/0.939 | $6.26 \times 10^{-8}$/0.925 | $7.21 \times 10^{-8}$/0.924 |
| $R_{p1}$(Ω) | 1050 | 678.9 | 487.2 | 358.1 | 261.1 |
| $CPE_2$:$Q_2/\alpha_2$ | $3.68 \times 10^{-8}$/0.840 | $2.78 \times 10^{-8}$/0.861 | $2.76 \times 10^{-8}$/0.861 | $2.67 \times 10^{-8}$/0.863 | $2.59 \times 10^{-8}$/0.864 |
| $R_{p2}$ (Ω) | 276.2 | 273.2 | 274.8 | 262.3 | 259.2 |

## 4. CONCLUSIONS

In summary, we have fabricated the simplified phosphorescent OLED devices comprising either a neat $MoO_x$ HIL or a $MoO_x$-doped CBP HIL. The devices having the $MoO_x$-doped CBP HIL are superior to the device having the neat $MoO_x$ HIL in terms of efficiency and lifetime. The IS studies have revealed that at least two factors contribute to the EL improvement. One is the reduced hole-injecting barrier height at the anode/doped HIL interface, and the other is the reduced bulk resistivity in the doped CBP HIL. When increasing the $MoO_x$ volume percentage from 5% to 20%, the hole-injecting barrier height is decreased from 0.63 to 0.18 eV. Comparing with the device having a neat $MoO_x$ HIL, the device having a 20 vol % of $MoO_x$-doped CBP HIL exhibits substantial power efficiency improvement and lifetime improvement. Therefore, the $MoO_x$-doped HIL can further improve the EL performance of the simplified PHOLEDs.

## ■ ASSOCIATED CONTENT

### Ⓢ Supporting Information

Device power efficiency versus $MoO_x$ doping concentration, current efficiency versus current density of the OLEDs (device series A), and photovoltaic IV charactersitics of the OLEDs (device series E). This material is available free of charge via the Internet at http://pubs.acs.org/.

## ■ AUTHOR INFORMATION

### Corresponding Author

*E-mail: lsliao@suda.edu.cn.

## ■ ACKNOWLEDGMENTS

We acknowledge financial support from the Natural Science Foundation of China (61036009, 61177016, and 21161160446), the National High-Tech Research Development Program (2011AA03A110), and the Natural Science Foundation of Jiangsu Province (BK2010003). This is also a project funded by the Priority Academic Program Development of Jiangsu Higher Education Institutions (PAPD).

## ■ REFERENCES

(1) Reineke, S.; Lindner, F.; Schwartz, G.; Seidler, N.; Walzer, K.; Lüssem, G.; Leo, K. *Nature* **2009**, *459*, 234−238.
(2) Kamtekar, K. T.; Monkman, A. P.; Bryce, M. R. *Adv. Mater.* **2010**, *22*, 572−582.
(3) Gather, M. C.; Köhnen, A.; Meerholz, K. *Adv. Mater.* **2011**, *23*, 233−248.
(4) Tao, Y. T.; Wang, Q.; Yang, C.; Qin, J.; Ma, D. G. *ACS Appl. Mater. Interfaces* **2010**, *2*, 2813−2818.
(5) Meyer, J.; Hamwi, S.; Bülow, T.; Johannes, -H. H.; Riedl, T.; Kowalsky, W. *Appl. Phys. Lett.* **2007**, *91*, 113506.
(6) Helander, M. G.; Wang, Z. B.; Qiu, J.; Greiner, M. T.; Puzzo, D. P.; Liu, Z. W.; Lu, Z. H. *Science* **2011**, *332*, 944−947.
(7) Wang, Z. B.; Helander, M. G.; Qiu, J.; Puzzo, D. P.; Greiner, M. T.; Liu, Z. W.; Lu, Z. H. *Appl. Phys. Lett.* **2011**, *98*, 073310.
(8) Adachi, C.; Kwong, R.; Forrest, S. R. *Org. Electron.* **2001**, *2*, 37−43.
(9) Malliaras, G. G.; Salem, J. R.; Brock, P. J.; Scott, J. C. *J. Appl. Phys.* **1998**, *84*, 1583−1587.
(10) Liao, L. S.; Ren, X.; Begley, W. J.; Tyan, Y. S.; Pellow, C. A. *SID'08 Dig.* **2008**, 818−821.
(11) Shin, W. J.; Lee, J. Y.; Kim, J. C.; Yoon, T. H.; Kim, T. S.; Song, O. K. *Org. Electron.* **2008**, *9*, 333−338.
(12) Tsang, S. W.; So, S. K.; Xu, J. B. *J. Appl. Phys.* **2006**, *99*, 013706.
(13) Hsieh, M. T.; Chang, C. C.; Chen, J. F.; Chen, C .H. *Appl. Phys. Lett.* **2006**, *89*, 103510.
(14) Ho, M. H.; Hsieh, M. T.; Lin, K. H.; Chen, T. M.; Chen, J. F.; Chen, C. H. *Appl. Phys. Lett.* **2009**, *94*, 023306.
(15) Tong, K. L.; Tsang, S. W.; Tsung., K. K.; Tse, S. C.; So, S. K. *J. Appl. Phys.* **2007**, *102*, 093705.
(16) Hsieh, M. T.; Ho, M. H.; Lin, K. H.; Chen, J. F.; Chen, T. M.; Chen, C. H. *Appl. Phys. Lett.* **2010**, *96*, 133310.
(17) Chen, C. C.; Huang, B. C.; Lin, M. S.; Lu, Y. J.; Cho, T. Y.; Chang, C. H.; Tien, K. C.; Liu, S. H.; Ke, T. H.; Wu, C. C. *Org. Electron.* **2010**, *11*, 1901−1908.
(18) Jonda, C.; Mayer, A. B. R. *Chem. Mater.* **1999**, *11*, 2429−2435.
(19) Kröger, M.; Hamwi, S.; Meyer, J.; Riedl, T.; Kowalsky, W.; Kahn, A. *Org. Electron.* **2009**, *10*, 932−938.
(20) Kröger, M.; Hamwi, S.; Meyer, J.; Riedl, T.; Kowalsky, W.; Kahn, A. *Appl. Phys. Lett.* **2009**, *95*, 123301.
(21) Meyer, J.; Shu, A.; Kröger, M.; Kahn, A. *Appl. Phys. Lett.* **2010**, *96*, 133308.
(22) Drechsel, J.; Pfeiffer, M.; Zhou, X.; Nollau, A.; Leo, K. *Synth. Met.* **2002**, *127*, 201−205.
(23) Meier, M.; Karg, S.; Riess, W. *J. Appl. Phys.* **1997**, *82*, 1961−1966.